TURBULENCE MEASUREMENTS IN STABLY STRATIFIED FLUIDS

BOEING SCIENTIFIC RESEARCH LABORATORIES

FEB 1970

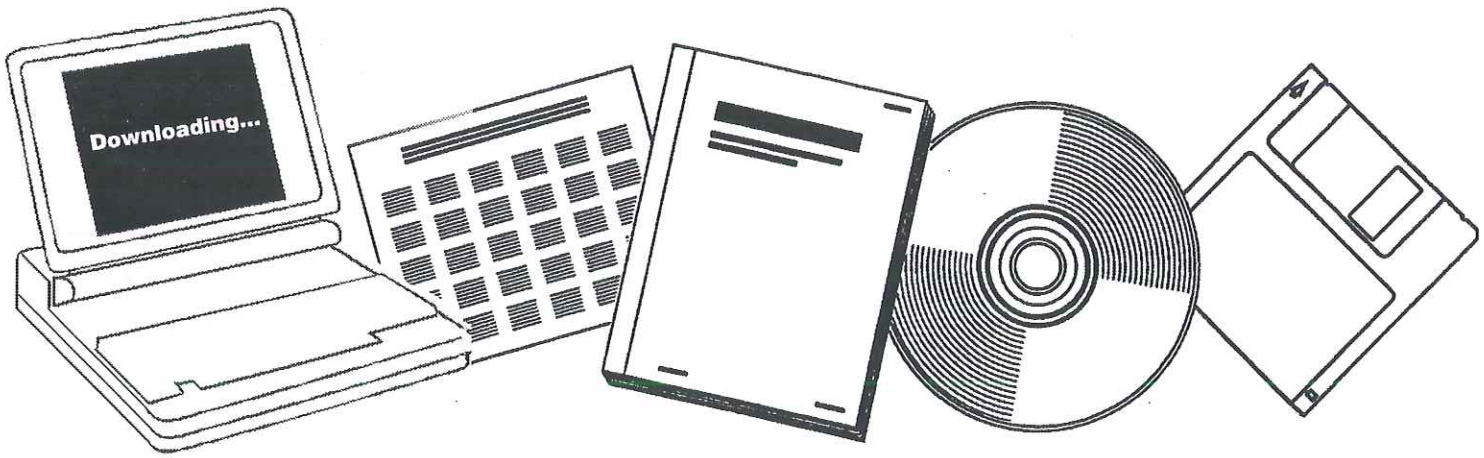

One Source. One Search. One Solution.

NTIS

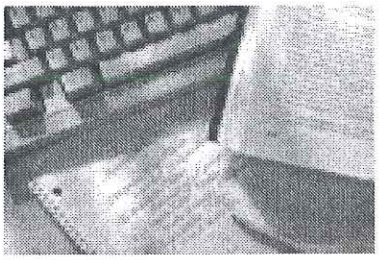

Providing Permanent, Easy Access to U.S. Government Information

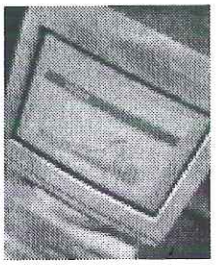

The National Technical Information Service is the Nation's largest repository and disseminator of government-initiated scientific, technical, engineering, and related business information. The NTIS collection includes almost 3 million information products in a variety of formats: electronic download, online access, DVD, CD-ROM, magnetic tape, diskette, multimedia, microfiche and paper.

Search the NTIS Database from 1990 forward

More than 600,000 government research information products have been added to the NTIS collection since 1990. All bibliographic entries for those products are searchable on the NTIS Web site at www.ntis.gov.

Download Publications (1997 - Present)

NTIS provides the full text of many reports received since 1997 as downloadable PDF files. When an agency stops maintaining a report on its Web site, NTIS still offers a downloadable version. There is a fee for each download of most publications.

For more information visit our website:

www.ntis.gov

U.S. DEPARTMENT OF COMMERCE
Technology Administration
National Technical Information Service
Springfield, VA 22161

D1-82-0959

FLIGHT SCIENCES LABORATORY

BOEING SCIENTIFIC RESEARCH LABORATORIES

TURBULENCE MEASUREMENTS IN STABLY STRATIFIED FLUIDS

by

Yih-Ho Pao

February 1970

TURBULENCE MEASUREMENTS IN STABLY STRATIFIED FLUIDS *

Yih-Ho Pao
Boeing Scientific Research Laboratories, Seattle, Washington 98124

Abstract

A towing tank system was used to study the structure of turbulence in stably stratified fluids. Turbulence is generated by moving an obstacle (a grid or a cylinder) in a tank of stratified salt water. Recent improved shadowgraph pictures of these laboratory generated stratified flows are shown in this paper. They give further support to Pao's (1969a) observation that (i) internal waves and turbulence coexist in turbulent stratified flows, with internal waves at the large scales and turbulence at the small scales; (ii) turbulence decays much more rapidly than internal waves; and (iii) the turbulent-nonturbulent interfaces are not necessarily sharp, and the transition region may consist of mostly internal waves.

Velocity and concentration fluctuations in the wake of the obstacle are measured respectively with quartz-coated hot-film probes and single electrode conductivity probes which are towed at the same speed as the obstacle. The velocity and concentration signals are processed with a digital computer utilizing a fast Fourier transform technique to obtain spectra, correlations, rms values, etc. Our probe

---

* An invited lecture delivered at the Symposium on Turbulence Measurements in Liquids, Rolla, Missouri, September 8-9, 1969.

measurement methods and data processing techniques will be discussed in detail in this paper.

The velocity auto-spectra measured behind the stratified wake of a cylinder behave like $f^{-5/3}$ for a decade of frequency range, although the turbulence Reynolds numbers are too low for the flows to have an inertial subrange. The reason for this anomalous inertial subrange is discussed in the context of a unified spectral model proposed by Pao (1969b). The measured concentration auto-spectra have a substantial range of frequencies behaving like $f^{-5/3}$; the $f^{-5/3}$ range of the concentration auto-spectra extend to higher frequencies than those of the velocity auto-spectra measured in the same position.

Diagnostic methods to distinguish internal waves from turbulence with two probe measurements are proposed. This can be accomplished by comparing the co-spectra and the quadrature-spectra or the coherencies of (i) two vertically separated velocity probes, or (ii) two vertically separated salinity (or temperature) probes, or (iii) a velocity probe and a salinity (or temperature) probe. These methods developed in the laboratory can be applied directly to atmospheric and oceanic measurements to distinguish internal waves from turbulence.

1. Introduction

Most of the atmospheric and oceanic motions are turbulent, and large portions of the atmosphere and ocean are stably stratified. Consequently, knowledge of the structure of turbulence in stratified fluids is necessary for a better understanding of our environment. There are different ways to gain this knowledge. An obvious way is through direct observation and measurement of various types of motions in a stably stratified atmosphere or ocean. This is usually costly and should be done very selectively. Furthermore, observational results and measurements obtained in uncontrolled natural conditions are often difficult to interpret. A second way is to isolate and to simulate the main features of these flows in laboratories, and to study them under controlled conditions with less cost and manpower. The study reported in this paper belongs to the second category.

Some preliminary results of our laboratory investigations of turbulence in stably stratified fluids were reported earlier (Pao, 1967, 1969a; Hall & Pao, 1969). By observing the generation and the decay of a patch of turbulence in a stratified liquid with the shadowgraph method, Pao (1969a) concluded that: (i) internal waves and turbulence coexist in these stratified flows, where internal waves predominate at the large scales and turbulence predominates at the small scales; (ii) turbulence decays much more rapidly than internal waves; and (iii) the turbulent and nonturbulent interfaces are not necessarily sharp, and the "transition" region may consist mostly of internal waves. Through some preliminary hot-film probe measurements Pao (1969a)

has compared the spectra of turbulence in stratified and nonstratified fluids, corresponding to the same turbulence generating conditions, and has shown that the spectra intensity was substantially less for the stratified case.

We have since improved our shadowgraph techniques and have observed visually the structure of turbulence in various kinds of stratified flows. These new shadowgraph pictures, which give further evidence of those characteristics described in the previous paragraph, will be shown and discussed in Section 5.

We have measured the velocity and salinity fluctuations in the stratifed wakes of a grid or a cylinder with quartz-coated hot-film probes and a single electrode conductivity probe. The obstacle (a grid or a cylinder) with the probes behind it is towed at a constant speed in a tank of stratified salt water (Fig. 1). The use of a towing tank system to study the stratified flow is not new. Long (1953, 1954, 1955) made a series of penetrating studies concerning stratified flows over barriers utilizing a towing tank system. Schooley and Stewart (1963) observed the collapsing of the turbulent wake of a self-propelled body and the induced internal waves in a tank. Kennedy and Froebel (1964), and Stockhausen, Clark, and Kennedy (1966) measured the mean velocity and concentration profiles of stratified turbulent wakes in a towing tank system. What is new and more demanding here is to utilize a towing tank system for turbulence measurements in stratified fluids. Our apparatus and instrumentation will be described in Section 2; our experimental procedures and data recording methods will be described in Section 3. Our data

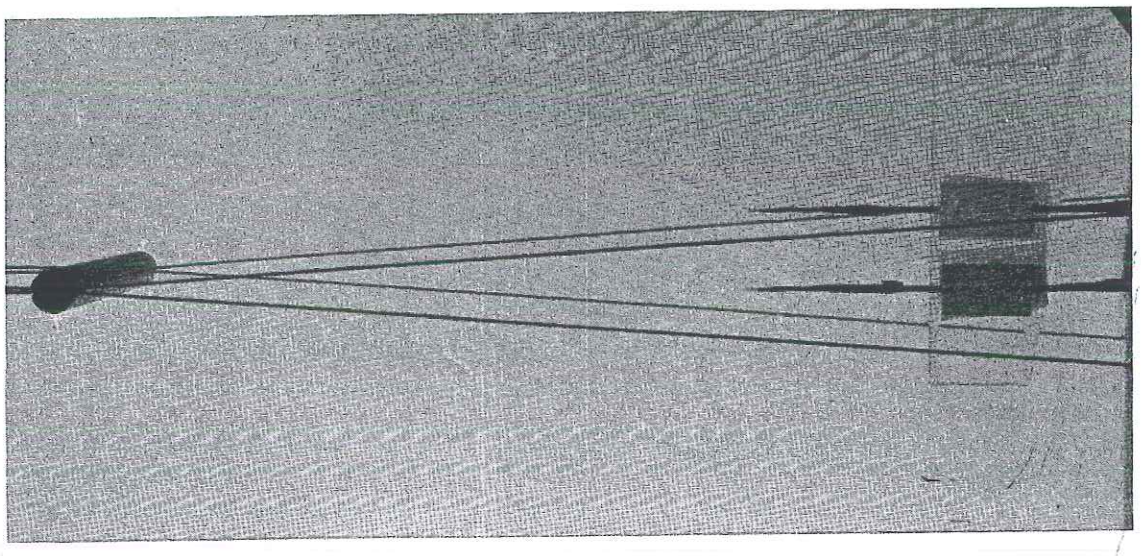

Fig. 1. A configuration for the circular cylinder and four probes (two Hot-film probes and two conductivity probes).

processing techniques will be described in Section 4. Our measured velocity and concentration auto-spectra will be described in Section 6. In Section 7, it is demonstrated that it is possible to distinguish internal waves from turbulence in a stably stratified fluid by comparing co-spectra and quadrature-spectra.

2. Apparatus and Instrumentation

There are a number of stringent requirements that we must meet in order to use the towing tank system successfully for turbulence measurements in stratified liquids. These requirements are: (i) The towing tank itself must be sufficiently long to provide enough averaging time for the statistical quantities of interest. To fill a long tank with salt water requires a large quantity of salt. The cost of each refill must be taken into consideration. (ii) Because of the vigorous turbulent mixing, the stratification is destroyed after each run. For an operational towing tank system, it is necessary to have a filling system that is capable of refilling the tank quickly according to a prescribed density profile. (iii) Hot-film probes are unable to distinguish probe vibrations from turbulence. Therefore, it is necessary to have a very smooth-moving carriage for the probes. (iv) In order to have meaningful quantitative results, the hot-film probes and the single electrode conductivity probes must be stable and drift-free. This is the most stringent requirement. We have been able to meet it only partially so far. (v) Because of the intermittent nature of these experiments and the difficulty in preparing each run, it is logical to use as many probes as possible for each run. This requires special data recording and data processing techniques which will be described in Sections 3 and 4 respectively. (vi) The structural support for the obstacle must be so small that it does not introduce extraneous effects into the wake.

After balancing the six requirements listed in the previous paragraph, with the funding and the space available at the time, we have

constructed a 35 ft. long towing tank system with an air-lubricated probe carriage. The system is designed in such a way that the probe carriage with quartz-coated hot-film probes and single electrode conductivity probes can be towed at the same speed as the obstacle. Signals from these probes are sent directly to an IBM 360-44 computer for direct on-line turbulence data processing or recorded on an FM magnetic tape for later processing. The details of the towing tank system and the probe measurement methods will be described below.

The Towing Tank is 35-feet long, 12-inches wide, and 30-inches high, (Fig. 2). It is made of aluminum struts with 1/2-inch thick plexiglass walls. The tank is sealed with silastics.

The Towing Mechanism consists of a driving drum (Fig. 3), a system of following pulleys, and nylon-coated stainless steel cables. The driving drum is made of aluminum machined to .001" accuracy, anodized to protect it from the salt water. The drum is powered by a 1/4 hp Boston-gear constant torque motor with Ratiotrol speed control. We have changed the control to a ten-turn pot to allow more refined speed adjustment. The center cable on the driving drum tows the air-lubricated probe carriage, and the outer four cables on the driving drum tow the obstacle(s). Each cable can be adjusted separately for the proper tension. A usual operating tension for the cable is 60 lb/in^2. The towing speed can be repeated with better than 0.3% accuracy (see Table 1 for an example). We have deliberately used the oversized driving motor to minimize the towing speed variation for each run; no variation can be detected within the accuracy of the hot-film anemometry.

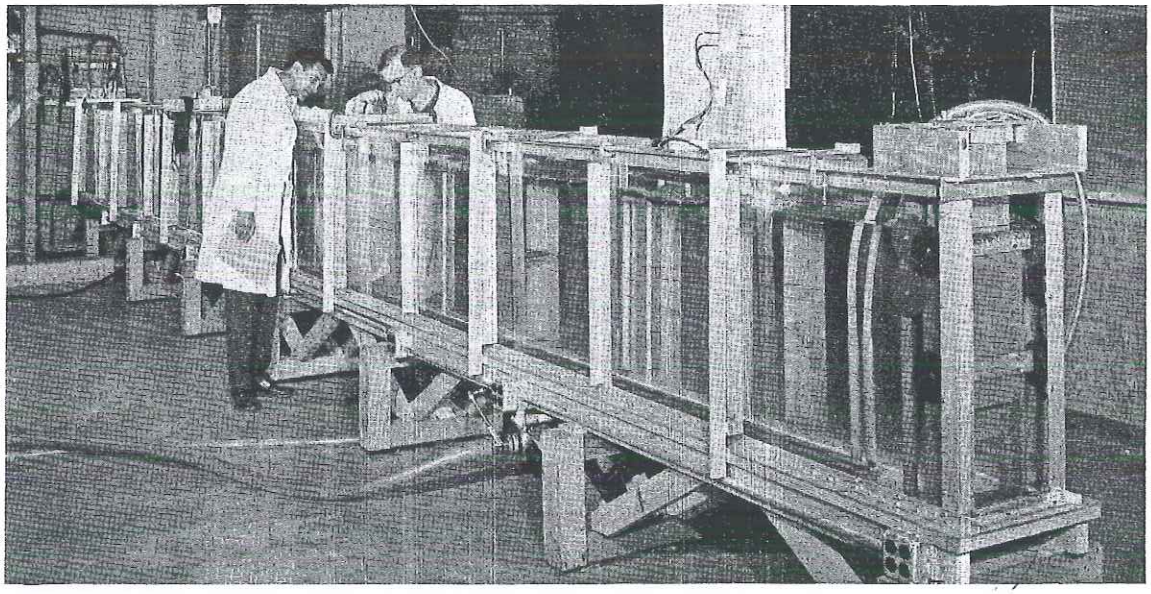

Fig. 2. The Towing Tank (35' long, 12" wide, and 30" high).

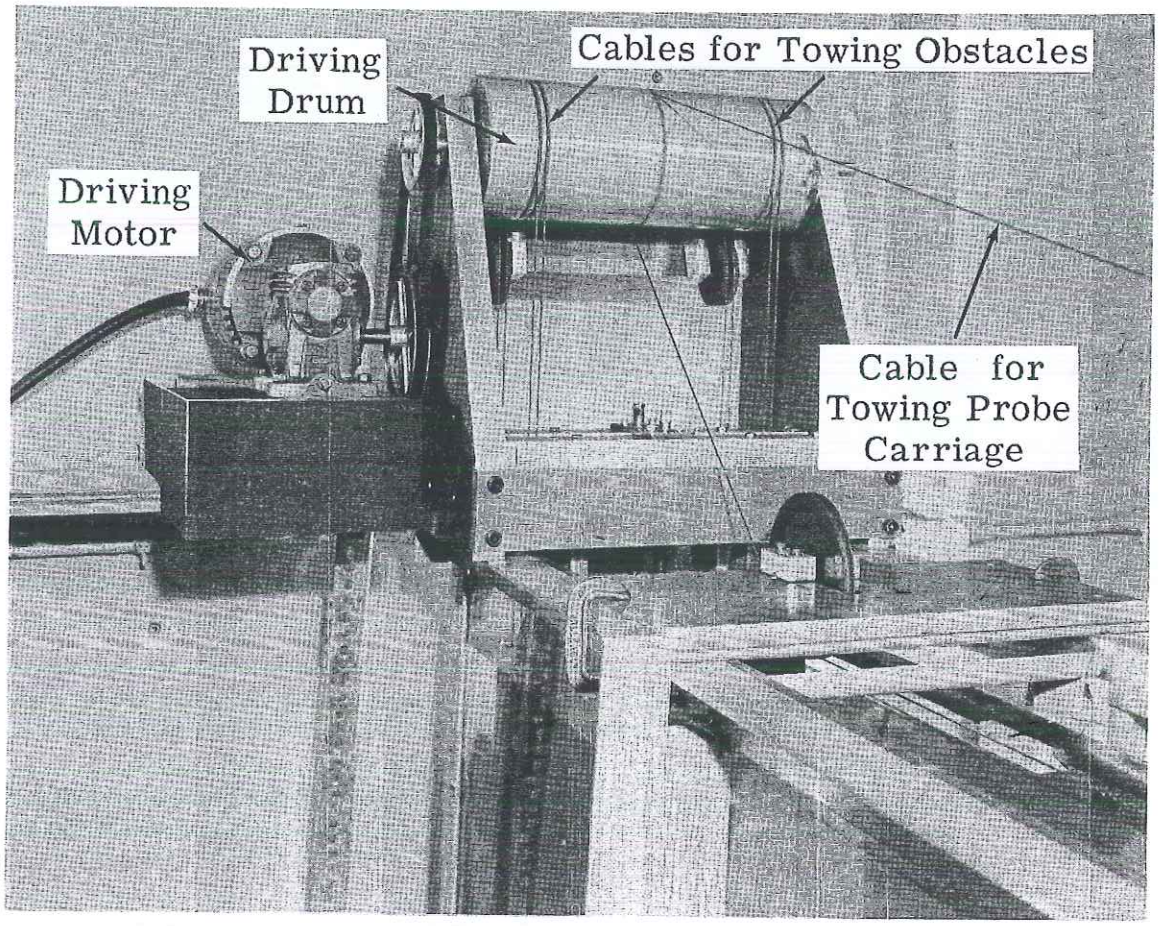

Fig. 3. The driving drum for the towing cables.

Preparation of the Fluids and the Filling System. Room temperature salt water is used as the working fluid. Two 500 gallon plastic storage tanks are used (Fig. 4). One tank is used to store tap water (part from the cold water line and part from the hot water line), and the other tank is used to store saturated salt water (the brine tank). These storage tanks are necessary for allowing the tap water to de-gas, because the small air bubbles in the water may attach to the hot-film probes and cause severe calibration drift. High purity table salt is first dumped into a small mixing tank and mixed with high velocity water jets. This saturated water is drained into the brine tank. There is a mechanical stirrer in the brine tank to assure the homogeneity of the brine. The filled storage tanks are allowed sufficient time (10 hours or more) to de-gas and to equilize their temperature with the room temperature. For each filling, the fresh water and the brine are pumped separately from the storage tanks to two elevated constant-head overflow tanks. Fresh and saturated salt water from these elevated tanks are fed into a mixing valve, where the mixing ratio, thus the density of the salt water, is controlled by a pressure valve. This salt water is fed by gravity force into the tank, layer by layer with increasing density through two feeding tubes at the bottom of the tank. These feeding tubes are 1-1/2" x 3/4" rectangular stainless steel tubes, stretched over the length of the tank, with small holes drilled at the bottom side. The feeding tubes rest on the bottom of the tank with 0.01" clearance; this appears to be effective in damping out the disturbances in the feeding stream and enables us to obtain a reproducible density stratification. The density distribution is simply determined by the pressure valve dial settings. The time required for each filling is about one hour.

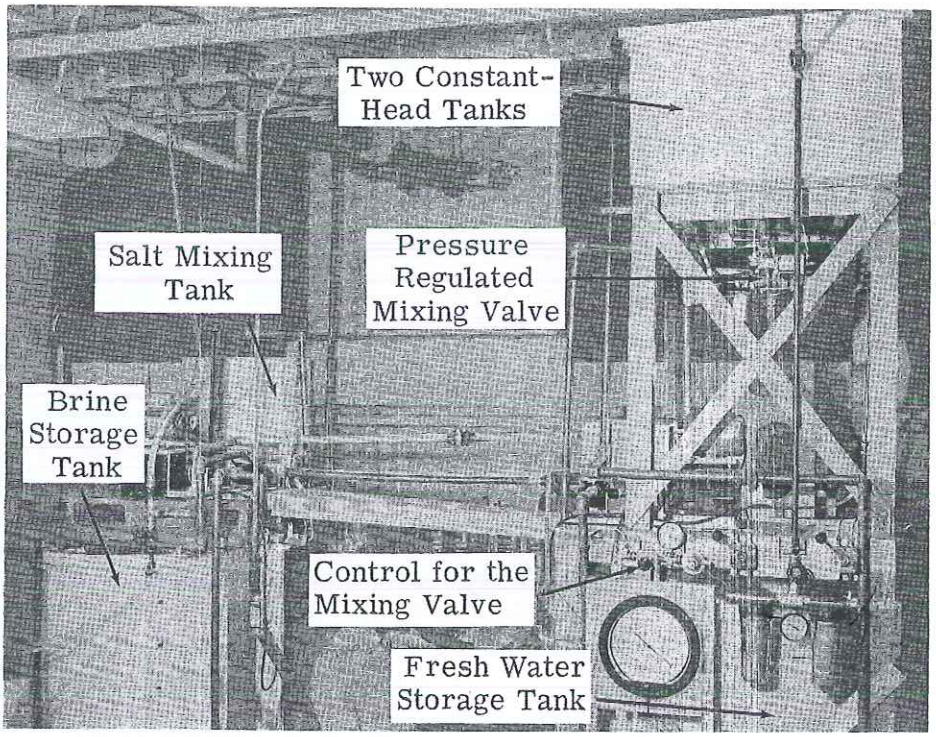

Fig. 4. A filling system for making the stratified salt water with a predetermined density gradient.

Probe Carriage. Because the hot-film probes can not distinguish carriage vibration from turbulence, we have spent a great deal of effort in developing a carriage that moves smoothly enough. We tried a carriage with rollers, a carriage with Teflon skids, and finally a carriage with air-lubricated shoes. These air-lubricated shoes ride on and are guided by two precision microwave-guide tubings. The air-lubricated carriage has reduced the probe vibration to an acceptable level. Table 2 shows the ratio of the rms velocity due to probe vibration, as recorded by a hot-film cone probe, to the mean velocity at various towing speeds. The operating air pressure is approximately 30 to 40 lbs/in^2.

Hot-Film Anemometry. The quartz coating seems to provide adequate electrical insulation for the hot-film from its surrounding liquid; it certainly is a major step toward the stable operation of hot-film probes in liquids. Looking back at some of our earlier data recorded in 1966 and 1967, when the quartz-coated hot-film probes were at their infancy and not well made, 10% drifts or greater in velocity calibration were common. Of course, the quartz coating does not eliminate all the problems with hot-film anemometry in liquids. In addition to the problems with suspended particles and fibers, hot-film measurements in liquids are sensitive to temperature changes due to the low overheat. Local boiling can occur at 60°C in water and at even lower temperature in salt water. Thus 60°C appears to be the upper limiting temperature for the hot-film. We have tried 5%, 7%, 10%, and 12% overheat ratio (overheat ratio r here

is defined as $r = (R_H - R_C)/R_C$, where R_H is the hot-film resistance and R_C is the cold film resistance) and found that 10% overheat ratio appears to be the optimal case. For our calibrated runs, we require the temperature variation to be within 0.1°F.

We have used mostly Thermosystems quartz-coated hot-film cone probes (1230G) in conjunction with Thermosystems 1054B linearized constant temperature anemometers to measure the streamwise velocity fluctuations. These cone probes are specially quartz-coated for salt water usage. We have found that the cone probe 1230W for water usage usually breaks down in salt water. We have experimented with the Thermosystems quartz-coated cylindrical hot-film probes (1270-10W, 1270-20W), and found that they have more calibration drift than cone probes. This is probably due to the particles and the fibres in the salt which can attach more easily to the cylindrical probes than the cone probes. It has been known for some time that the larger size (.06" diameter) cylindrical hot-film probes will be more stable than the smaller ones, but we have not used the larger cylindrical probes (1270-60W) because we expect the vortex shedding problems cited by Fabula (1968). Because of the probe carriage vibration, we have ruled out the possibility of using wedge probes which are extremely sensitive to the angle of attack.

To improve the water quality, we have a re-circulating system which will continuously circulate the water in the tank through a series of mechanical filters (the last one in the series is a 1-μ particle filter). With this recirculating system, we can repeat our calibration in water with less than 1% deviation.

We have operated the Thermosystems 1054B hot-film anemometers in the ordinary and the linearized mode. We found the cone probes do not obey the generalized King's law over a broad range of speed variation although it is possible to fit the King's law to a narrow range of speed. We have derived a method to send our velocity-voltage calibration directly to a computer; the calibration points are fitted with a sixth-order Chebychev polynomial by the computer. The voltage read by the computer is converted to the velocity accordingly. The details of this method will be discussed in Section 4.

The Single Electrode Conductivity Probes that we have used are the same in principle as the ones developed by Gibson and Schwarz (1963). The method we used to construct the probe is very simple. Our conductivity probes are constructed from stainless steel needles coated with epoxy. First, the epoxy is mixed and thinned down by heating. Then, the stainless steel needles are dipped into the heated epoxy. After the epoxy is set, the tip of the needle is ground to expose the stainless steel. The exposed portion is then coated with the platinum black to increase its corrosive resistivity. The conductivity probe is used in conjunction with a modified Tektronix 3C66 or Q plus-in unit, which is a carrier amplifier. The system has good sensitivity and is capable of measuring salinity variation as little as 0.01%. One of the problems with this system is the drift, mostly due to the electronics. We are in the process of developing a solid state circuit for conductivity measurements. The signals from the single electrode conductivity probes are converted by the computer to density again through the fitting of the density-voltage calibration points with a sixth-order Chebychev polynomial.

Obstacles. The obstacles that we have used are either a neutrally buoyant grid or a neutrally buoyant circular cylinder. The four corners of the grid or the ends of the circular cylinder are attached to tightly stretched Nylon coated stainless steel cables. These cables are towed by the driving drum. The grid is made of 3/8" or 3/16" plexiglass tubing. The mesh to diameter ratio is 5.33. The circular cylinder is made of 3/4" or 1" plastic tubing. To make these obstacles neutrally buoyant, proper weights are inserted into these tubings whose ends are then sealed.

3. Experimental Procedure and Data Recording

The day before the run, the fresh water and the brine in the storage tanks are prepared as described in Section 2. Before the run, we first check the temperature of the liquids in the two storage tanks to make sure they are the same as the room temperature. Then the obstacle and the good probes are put in the proper places. Then the tank is filled with stratified salt water, which takes about an hour. After the tank is filled, we turn the hot-film anemometers and the Q units on to see if there are any problems with the probes. In our experiments we have used two vertically separated hot-film probes and two vertically separated single-electrode conductivity probes. Signals from these four probes are recorded on FM magnetic tapes with a 14-channel Ampex FR-1300 FM magnetic tape recorder at 15 ips tape speed. The 15 ips tape speed gives a flat frequency response from 0 to 5000 Hz. The signals from the four probes often exceed the input voltage range (±1.414 volts) of the FM tape recorder and need to be attenuated with preamplifiers. These four attenuated signals are recorded in four channels on the FM tapes (for convenience, we call these channels the D.C. channels). We are interested in obtaining the mean and the fluctuating components. The fluctuating components can, in principle, be obtained from the D.C. channels. However, because of the limited dynamic range of the magnetic tape recording system, it is advantageous to record the fluctuating components separately. This is done by sending the signals through band-pass filters, D.C. amplifiers, and then recording them on four separate channels (for convenience, these are called the A.C. channels).

The instrumentation flow diagram is shown in Fig. 5.

Before each run, we estimate the level of the signals; the preamplifiers and amplifiers will be set accordingly. Then standard reference signals of 0, + 200 mv, and -200mv are injected into all channels. We are then ready to record an actual run, which is usually rather short, ranging from 10 sec to 1 min. After the run, we take the obstacle out and run the probes in a quiescent tank at various speeds to calibrate the hot-film probes. After the hot-film probe calibration, we take the single-electrode conductivity probes out and dip them into our standard density jars for calibration. These two calibrations are also recorded on tapes. These signals are then sent through coaxial cables to an IBM 360-44 digital computer with an IBM 1827 analog-to-digital converter for digital turbulence data processing.

Instead of recording all the signals on magnetic tape, we can send these signals directly to the IBM 360-44 computer for the direct-on-line turbulence data processing which enables us to examine our measurements in situ and yields considerably better signal to noise ratio. The details of the data processing technique will be described in the next section.

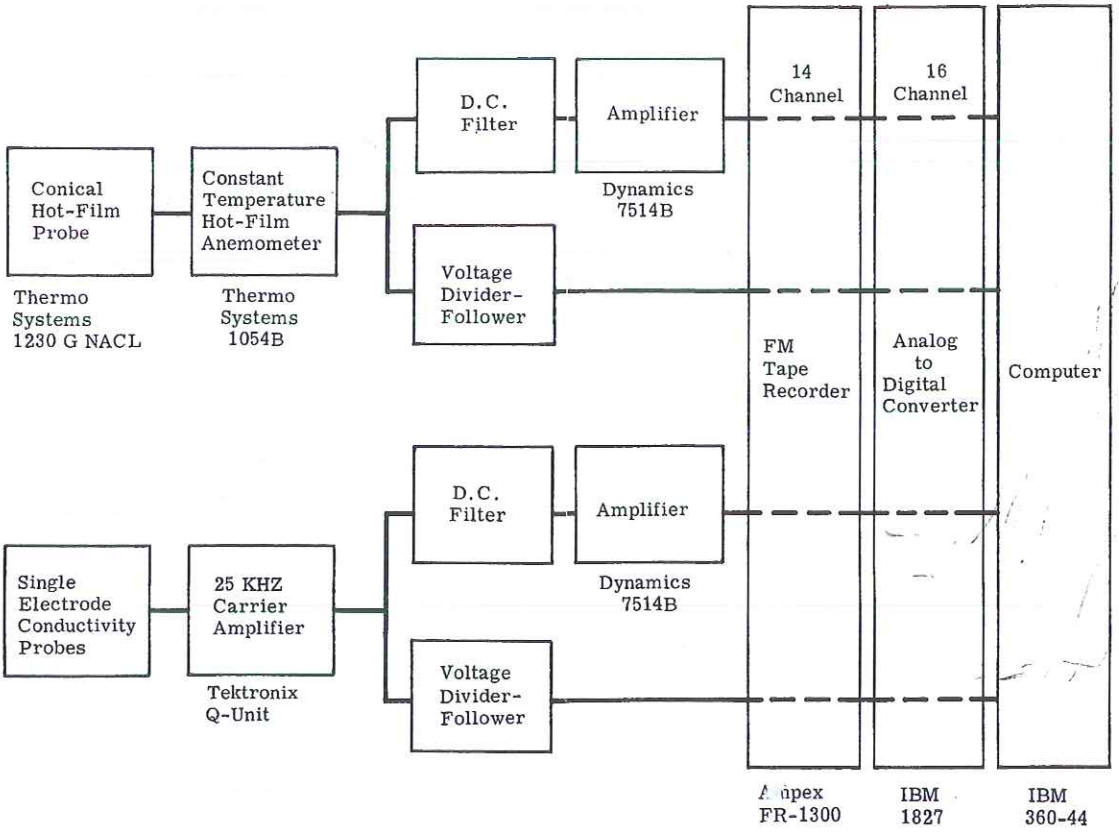

Fig. 5. Instrument flow diagram.

4. Data Processing Technique

Turbulence signals are sent by coaxial cables (approximately 300 ft long) to an IBM 1827 analog-to-digital converter, which has a 16-channel multiplexer and a conversion rate of 18,000 samples per second at 15 bits (including the sign bit) accuracy. The digitized data are then processed with an IBM 360-44 computer with 32,000 words core memory. A computer program for dual channel data processing (PAϕ-K) utilizing the fast Fourier transform algorithm is developed to handle the fluctuating signals from two probes (A.C. channels). This program (PAϕ-K) is an extension and modification of an earlier program (PAϕ-J) developed by Pao, Hansen, MacGregor (1969). It yields rms values, auto-correlations, cross-correlations, auto-spectra, cross-spectra, phase angles, co-spectra, quadrature spectra, and coherencies. This program (PAϕ-K) consists of four subprograms: 1) RESIG - this subprogram accepts reference signals such that amplification and attenuation can be properly accounted for, and punches out cards for proper conversion factors. 2) CALIB - this subprogram accepts calibration runs for velocity and salinity probes, and punch-out cards for the calibration points to be inserted in the subprogram FIT. 3) FIT - the calibration points for the velocity and/or the salinity probes will be fitted by sixth-order Chebychev polynomials. The coefficients of these polynomials are punched out in cards to be inserted in the subprogram SPECTRA. 4) SPECTRA -- This subprogram accepts turbulence signals from two channels, converts them according to the fitted calibration curves, and computes with the fast Fourier transform algorithm the statistical quantities mentioned previously.

5. Structure of Turbulence in Stratified Fluids as Observed from the Shadowgraphs

From a sequence of shadowgraph pictures of laboratory generated turbulent stratified flows, Pao (1969a) observed that (i) internal waves and turbulence coexist in turbulent stratified flows, with internal waves at the large scales and the turbulence at the small scales; (ii) turbulence decays much more rapidly than internal waves; (iii) the turbulent-nonturbulent interfaces are not necessarily sharp, and the transition region consists of mostly internal waves. These conclusions will be further supported by recent improved shadowgraph pictures for various flow configurations to be discussed in the following paragraphs.

Figure 6 is a sequence of shadowgraph pictures showing the generation (Fig. 6a) and the decay (Fig. 6b,c) of internal waves and turbulence in stably stratified salt water. The cylinder is moving while the camera is stationary. Fig. 6a shows the region where the internal waves and turbulence are generated by the moving cylinder. Although Fig. 6a does not show any distinct wave behavior, one can infer from shadowgraph pictures taken at subsequent times (Fig. 6b and c) that there must be internal waves imbedded in the apparent turbulent structure in Fig. 6a. This is possible because the turbulence decays much faster than internal waves as is evident from Fig. 6b, which was taken at 14.2 sec. later. The cylinder has moved 102 cm away from the left edge of the picture. Fig. 6b shows the distinct wave

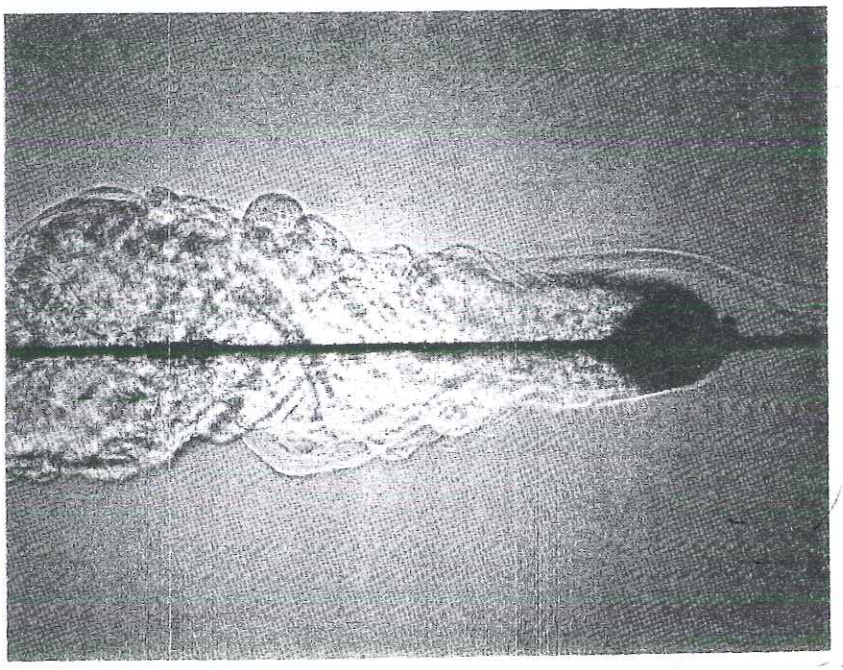

Fig. 6. a) The generation of internal waves and turbulence by a moving circular cylinder in a stably stratified salt water (shadowgraph). Cylinder Diameter D = 1.905 cm, Towing Speed $U = 7.226$ cm sec^{-1}, Specific Gravity Gradient $\gamma = .00255$ cm^{-1} $Re = UD\nu^{-1} = 1376$. $Ri_D = \rho_o^{-1} g\gamma D^2 U^{-2} = 0.154$. Brunt-Vaisala frequency $f_B = 0.237$ HZ.

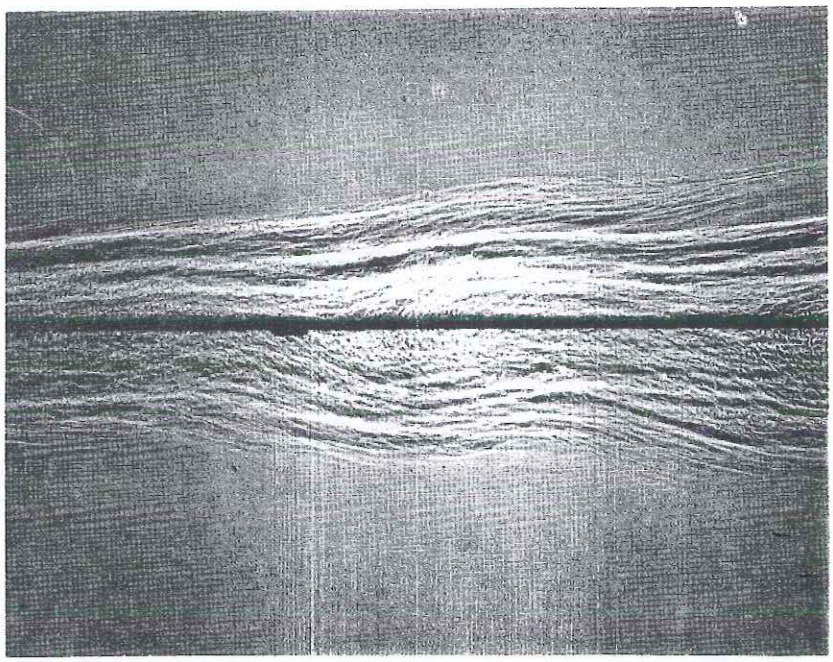

b) The decay of turbulence in the stratified wake of a circular cylinder (shadowgraph). This picture was taken at 14.2 sec after Fig. 6a where the cylinder was moved approximately 102 cm to the left edge of picture.

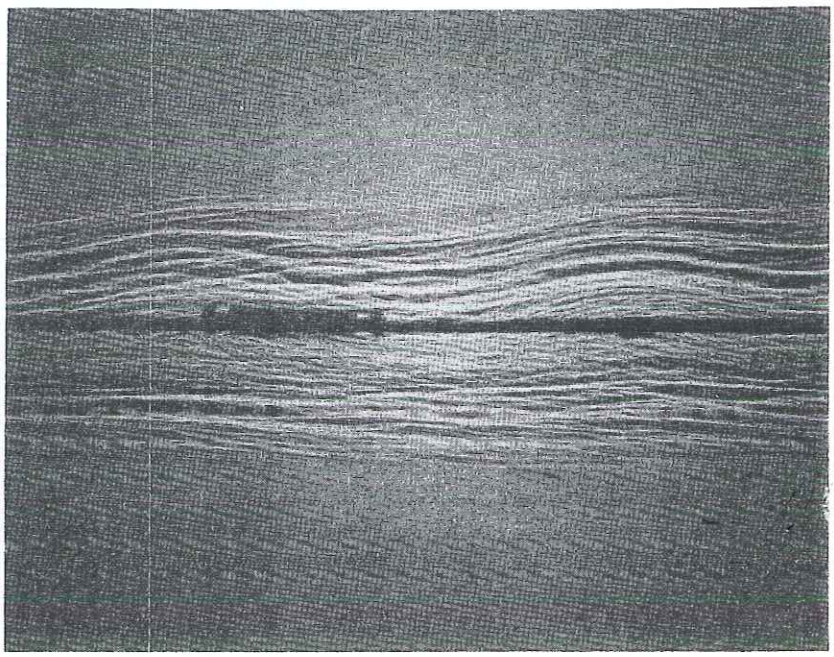

c) The decay of turbulence in the stratified wake. This picture was taken at 30.0 sec after Fig. 6a, where the cylinder was moved approximately 209 cm to the left edge of the picture.

behavior at large scale and turbulence behavior at small scale. Figure 6c was taken at 29.0 sec later. The cylinder has moved 209 cm away from the left side of the picture; it shows that turbulence has nearly all decayed away and the long wavelength internal waves are prevalent. This sequence of improved shadowgraph pictures, corresponding to earlier shadowgraph pictures shown by Pao (1969a, Figures 11 and 12) give further support to Pao's (1969a) observation that: (i) internal waves and turbulence coexist in turbulent stratified flows, with internal waves predominating at large scales and turbulence predominating at small scales, and (ii) turbulence decays much more rapidly than internal waves. The latter observation is analogous to the phenomenon commonly called the permanence of big eddies in homogeneous fluids, where small eddies decay much faster than big eddies. In turbulent stratified flows, the "big eddies" are the internal waves.

When the turbulence is first generated, Fig. 6a, the turbulent-nonturbulent interfaces are sharp and distinct which indicates sharp changes in refractive indices, hence, densities. This can be seen more clearly from a close-up of the turbulence generating region, Fig. 7a. When the turbulence is decaying (Fig. 6b), however, the turbulent-nonturbulent interfaces are no longer distinct. This can be seen more clearly from a close-up view shown in Fig. 7b. There are internal waves present between the turbulent and the nonturbulent regions. This gives further support to Pao's (1969a) observation that (iii) the

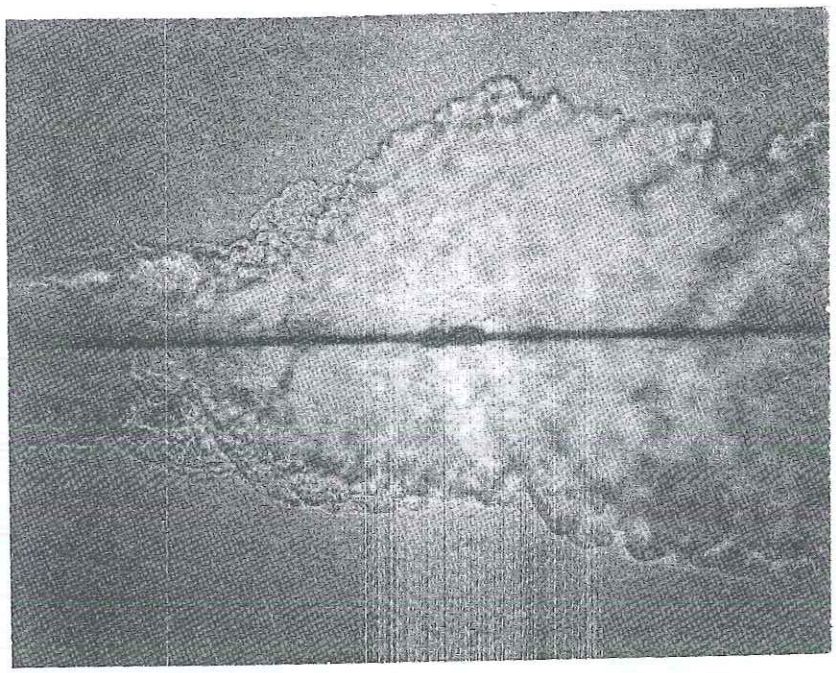

Fig. 7. a) Close-up view of turbulence generating region of a wake (see Fig. 6a for detailed description).

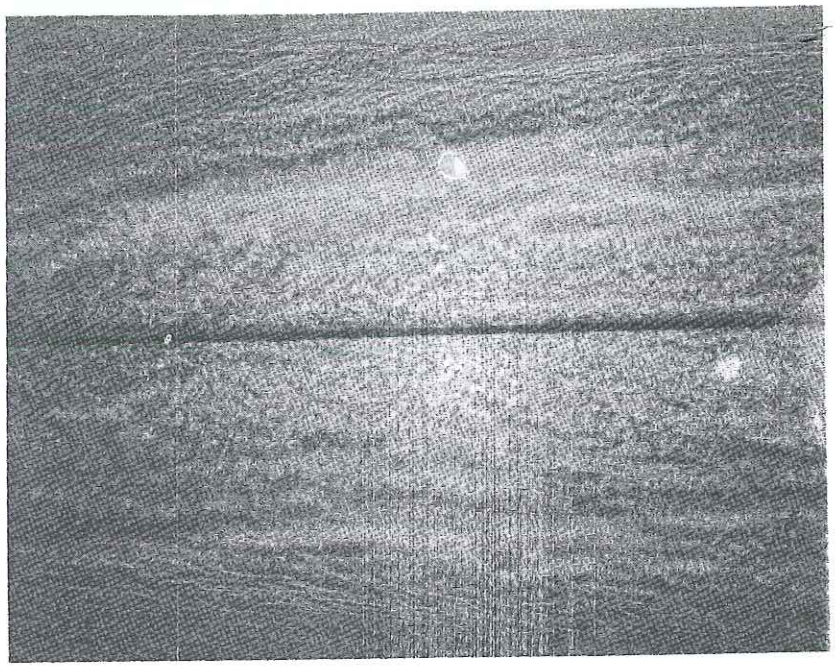

b) Close-up view of the turbulence decaying region of a wake (see Fig. 6b for detailed description).

turbulent and nonturbulent interfaces are not necessarily sharp, and there may be internal waves present in the "transition" region. The presence of these internal waves, we believe, is a part of the decaying process. The sharp density gradients at the turbulent-nonturbulent fronts yields a strong mechanism to suppress turbulence. This causes the turbulence to decay more rapidly than internal waves in the frontal regions.

The behavior at the turbulent-nonturbulent fronts, we believe, is of importance to the detection of clear air turbulence through the refractive-index fluctuation by ground-based sensitive radar [e.g., Hardy et al (1969)]. In the turbulent generating region, the sharp refractive-index gradients at the frontal surfaces may yield strong radar echoes even for weak turbulence. In the turbulence decaying regions, on the other hand, the lack of sharp turbulent-nonturbulent fronts (thus, the lack of sharp refractive-index gradients), may yield weak radar echoes even for relatively strong turbulence. This argument, of course, is no more than a plausible reasoning at the present time. Quantitative measurements are needed to carry this argument any further.

Figures 8 a and b are shadowgraph pictures showing respectively the generation and the decay of turbulence behind a moving grid. Figure 8b was taken at 27.4 sec later than Fig. 8a and the grid was approximately 177.8 cm away from the left edge of the picture. Fig. 8b shows the nearly homogeneous structure of internal waves where the turbulence has decayed away. This again supports Pao's (1969a) observation that turbulence decays much

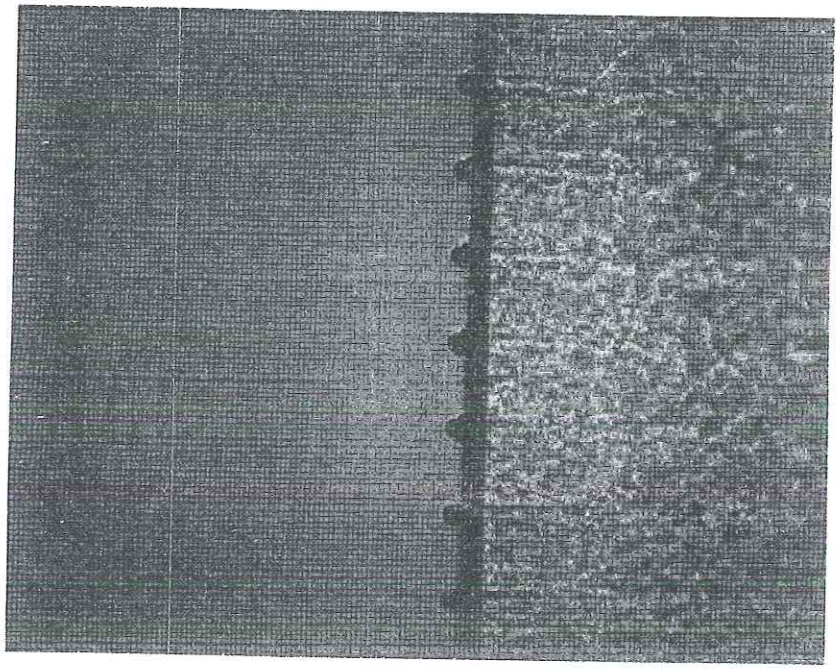

Fig. 8. a) The generation of internal waves and turbulence by a moving grid in a stably stratified salt water (shadowgraph). Grid tubing diameter = .476 cm, Grid mesh size M = 2.54 cm, Towing speed U = 6.48 cm sec^{-1}. $\gamma = 0.00335$ cm^{-1}. $Re_M = UM\nu^{-1} = 1650$, $Ri_M = \rho_o^{-1} g\gamma M^2 U^{-1} = .462$. $f_B = 0.276$ Hz.

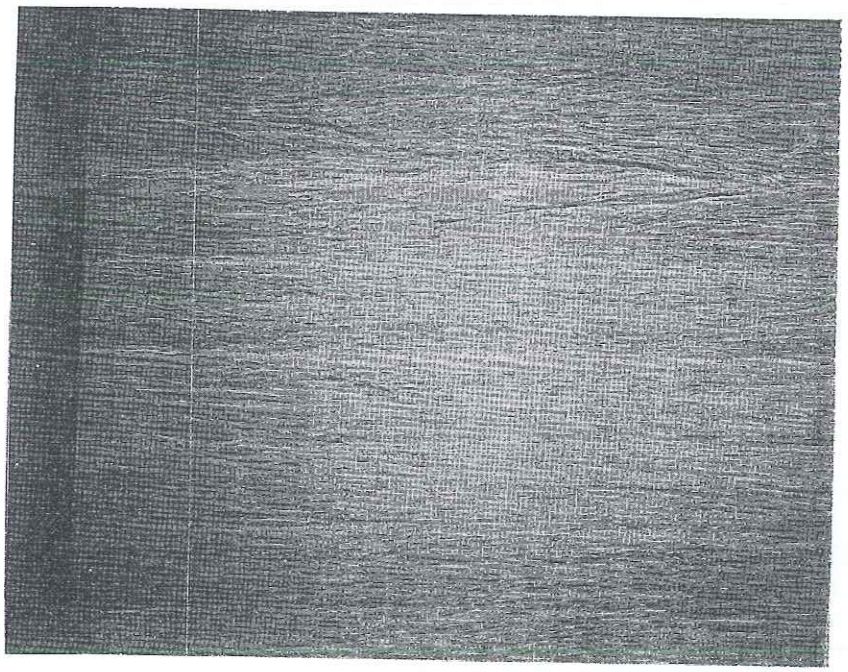

b) The decay of turbulence in the stratified wake of a grid (shadowgraph). This picture was taken at 27.4 sec after Fig. 8a, and the grid was moved approximately 178 cm to the left edge of the picture.

6. Velocity and Concentration Auto-Spectra

From a series of laboratory experiments (Pao 1967, 1968c, 1969a; Hall & Pao, 1969; and measurements in this paper), analyses (Pao 1965, 1968a, b), and existing atmospheric and oceanic measurements, Pao (1969b) proposed a unified auto-spectral description for internal waves and turbulence in a stably stratified fluid. Pao (1969b) proposed that, for sufficiently high Reynolds numbers and Richardson numbers, the spectral behavior of the fluctuating motion in a stably stratified fluid can be described in terms of four subranges, Fig. 9: (1) Internal Wave Subrange - the internal waves predominate at low wavenumbers (see Fig. 9). When the internal waves are sufficiently strong and distinct, the different harmonies of internal waves may present themselves as peaks in the auto-spectra. This behavior is predicted by Pao (1968b) in examining analytically the velocity and temperature spectra in the locally homogeneous range of wavenumbers based on the complete set of two-point covariance equations. It is also born out in a laboratory experiment by Hall and Pao (1969) on the breaking of internal waves in a two-fluid system. This is believed to be the reason (Pao, 1969a) for the presence of peaks and valleys in some auto-spectra, measured in stably stratified atmosphere and ocean, where the peaks represent different harmonics of the internal waves. When the internal waves are neither strong nor distinct, they can be identified through their co- and quadrature-spectra. This diagnostic technique will be described in Section 7. (2) Buoyant Subrange - the buoyant effect and turbulent scrambling effect are both important at intermediate wavenumbers where the high-order harmonics of internal

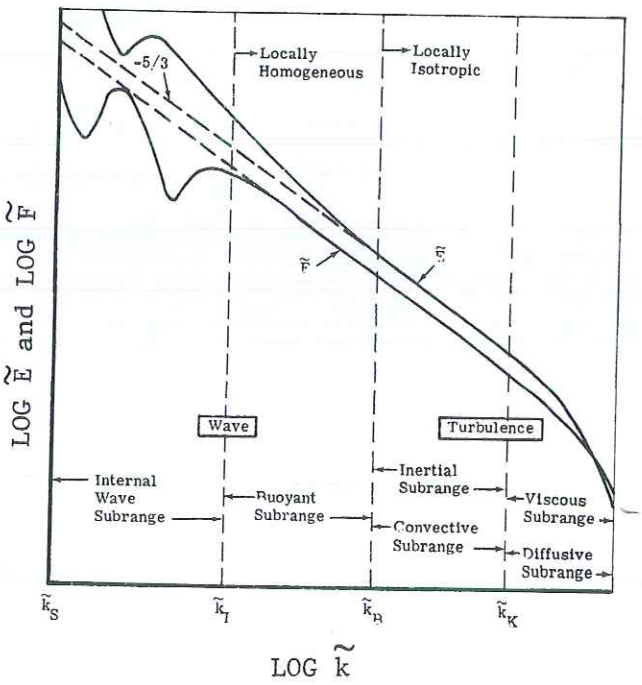

Fig. 9. A unified spectral description for internal waves and turbulence in a stably stratified atmosphere. All quantities are made dimensionless with governing parameters at small scales: ε, χ, ν and κ. $\tilde{k}_S$ is the wavenumber corresponding to the synoptic scale motion. $\tilde{k}_I$ is the wavenumber below which internal waves predominate. $\tilde{k}_B$ is the wavenumber beyond which turbulence predominates. $\tilde{k}_K$ is the Kolmogorov wavenumber beyond which the viscous and diffusive effects become important (after Pao, 1969b).

waves, if present at lower wavenumbers, are no longer distinct and can not be detected in the auto-spectra; this range of wavenumbers may be called the buoyant subrange. This definition covers a broader wavenumber range than the "buoyant subrange" defined by Bolgiano (1959, 1962). Pao (1968b) predicted the velocity and scalar spectra in this subrange do not obey any power law where the velocity spectra are steeper than $\tilde{k}^{-5/3}$, and the scalar spectra are less steep than $\tilde{k}^{-5/3}$. At higher wavenumbers, turbulence predominates. The fluctuating motion at these high wavenumbers are not affected by the stratification and can be described well with Kolmogorov's (1941) concept of local isotropy. Following Kolmogorov, the high wavenumber range can be divided into two subranges: (3) Inertial Subrange (convective subrange for the scalar quantity such as concentration or temperature); (4) Viscous Subrange (diffusive subrange for the scalar quantity).

Pao (1969b) has pointed out that the presence of these four subranges will depend on the Reynolds number and the Richardson number for a given flow. For flows with relatively low Reynolds numbers and high Richardson number the internal wave subranges (possibly with spectral peak or peaks) is very near the viscous subrange. Our laboratory generated stratified flows belong to this case. We shall present some of our measured autospectra in the context of the unified spectral model (Pao 1969b) briefly reviewed in the previous paragraphs.

Two velocity auto-spectra measured in the wake of a circular cylinder with a conical hot-film probe V4 are shown in Figure 10 -- a stratified case (WSL-5) and a non-stratified case (W-12). The data represented by open circles (W-12) were measured in water with a hot-film

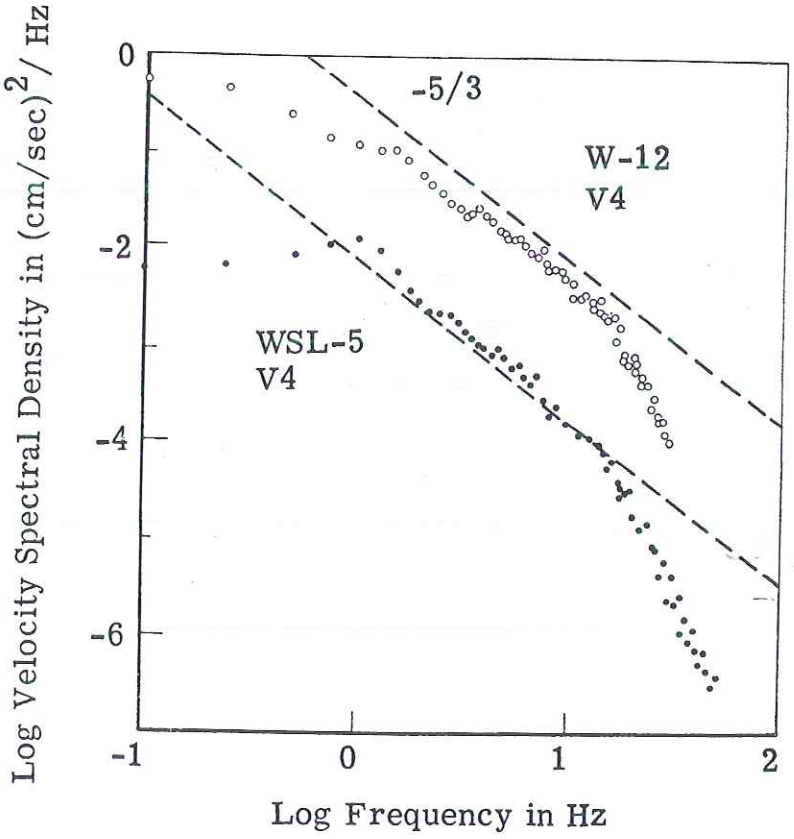

Fig. 10. Velocity auto-spectra in the wake of a cylinder. Cylinder diameter D = 2.54 cm. Position of the hot-film probe V4 is x = 50.8 cm downstream of the cylinder (x/D = 20). Vertical distance from wake axis is z = 2.54 cm (z/D = 1).

○ Velocity auto-spectra in a homogeneous fluid. (Run W-12, probe V4). Re = 4210. U = 16.594 cm/sec.

● Velocity auto-spectra in a stably stratified fluid (Run WSL-5, probe V4). Re = 4120. Ri = .0688. Sp. Gr. Grad. $\gamma = 3.213 \times 10^{-3}$ cm^{-1}. U = 16.208 cm/sec. f_B = 0.266 Hz.

probe V4 at 20 diameters behind the cylinder (x/D = 20) and one diameter above the wake-axis (z/D = 1). The Reynolds number Re (=UD/ν) based on the towing speed U and the cylinder diameter D is Re = 4210. The auto-spectrum behaves like $f^{-5/3}$ for about a decade in the frequency range. The data represented by the solid circles (WSL-5) were measured in stratified salt water with the same probe at the same position. The specific gravity gradient of the salt water was $\gamma = \rho_w^{-1}|d\rho/dz| = 3.213 \times 10^{-3} cm^{-1}$. ρ_w is the density of water at 4°C. The Richardson number $Ri = \rho_o g\gamma D^2/U^2 = 0.0688$, where ρ_o is the upstream density along the wake axis. The Reynolds number Re = 4120, very close to that of Run W-12. However, the auto-spectral density of the stratified case is nearly two decades lower than that of the non-stratified case. It shows a spectral peak close to the Brunt-Väisälä frequency of the stratified salt water, $f_B = (g\rho_o\gamma)^{1/2}\, 2\pi^{-1} = 0.266$ Hz, and has a distinct $f^{-5/3}$ frequency range. However, the turbulence is too weak to have a distinct $f^{-5/3}$ inertial subrange. This "anomalous inertial subrange", we believe, is due to the presence of the internal wave spectral peak and lifted the spectral curve up as a result.

The result described in the previous paragraph should be considered as a caution flag to those who derive turbulent energy dissipation rate ε from spectra measured with relatively slow response instruments (such that ε can not be measured directly). This is commonly done with atmospheric data. The procedure is to assume Kolmogorov's Law for the inertial subrange

$$\phi = \alpha\varepsilon^{2/3} k^{-5/3}$$

where α is Kolmogorov's universal constant, k is the wavenumber and can be

related to the frequency by Taylor's hypothesis, $k = 2\pi f/U$. ε is then calculated from the measured velocity spectral density ϕ, provided that the spectrum has a distinguishable $k^{-5/3}$ range. However, our results (Fig. 10) show that the presence of the $f^{-5/3}$ frequency range does not warrant the existence of inertial subrange in a stably stratified fluid.

A velocity and a concentration spectra measured respectively with a hot-film probe V4 and a single electrode conductivity probe C3 in the stratified wake are shown in Fig. 11 (Run WSF-2, Re = 4325, Ri = 2.424). The salt water was strongly stratified and f_B = 1.66 Hz, γ = 0.12 cm^{-1} in this run. In order to achieve this strong stratification with salt, we have limited the vertical extent of the stratified region to 10.16 cm, with fresh water above and saturated salt water below. The cylinder was placed at the middle of the stratified region. The velocity spectrum measured with the hot-film probe V4 at one diameter above the wake axis (z/D = 1) is shown in solid circles in Fig. 11. It again has a $f^{-5/3}$ range. The concentration spectrum measured with the single electrode conductivity probe C3 placed on the wake axis (z/D = 0) is shown in open circles in Fig. 11. It has a strong spectral peak near the Brunt-Väisälä frequency of the stratified salt water (f_B = 1.66 Hz). It also has a $f^{-5/3}$ range, which extends to much higher frequencies than those of the velocity autospectra.

In an experiment on the breaking of internal waves in a two fluid system (Hall & Pao, 1969) we have shown that in these breaking waves the different harmonics of the finite amplitude internal waves present themselves in the frequency auto-spectra of wave height as spectral peaks. In this section, we have further shown that the velocity

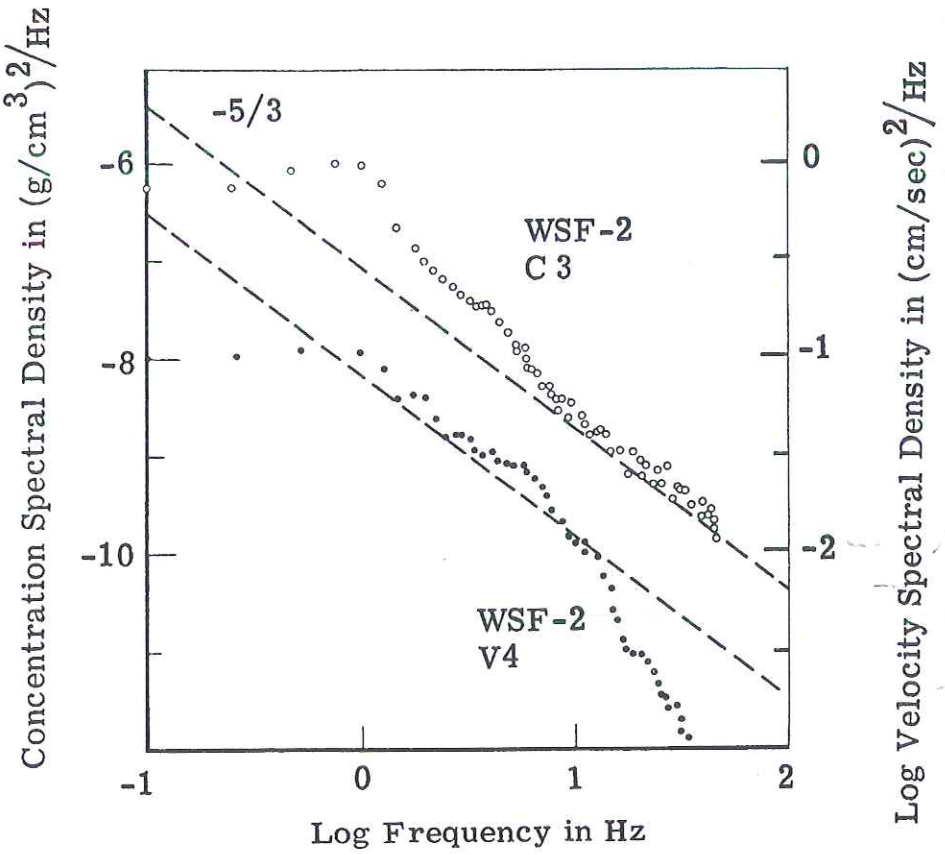

Fig. 11. Velocity and concentration auto-spectra measured in the wake of a circular cylinder in a stably stratified fluid. (Run WSF-2). Cylinder diameter D = 2.54 cm. The probe V4 is placed at x/D = 20 and z/D = 1. The probe C3 is on wake axis z/D = 0. The horizontal distance between C3 and V4 is 1.7 cm. The vertical distance between V4 and C3 is 2.54 cm. Re = 4325. Ri = 2.424. $\gamma = 1.2 \times 10^{-1} cm^{-1}$. f_B = 1.66 Hz.

○ concentration auto-spectrum

● velocity auto-spectrum

and/or concentration auto-spectra may also have peaks in a continuously stratified turbulent flow.

7. Co-spectra and Quadrature-spectra as Diagnostic Tools in Distinguishing Internal Waves from Turbulence

In a turbulent stratified fluid, when the auto-spectra do not have distinct peak or peaks, as is the case with the auto-spectrum WSF-2, V4 in Fig. 11, the internal wave subrange can be identified from the co- and quadrature spectra of two vertically separated probes or of a velocity probe and a concentration probe at the same height. The underlying assumptions are: (1) the turbulence is a strong interaction phenomena and has very weak phase relation between measurements at two points, while the internal waves are a weak interaction phenomenon and have strong phase relation between measurements at two points; (2) turbulence can only be convected by the stream and does not propagate, while internal waves can propagate, while internal waves can propagate in the vertical direction. If these assumptions are correct, they imply that in a turbulent homogeneous flow (with no internal waves present), the velocity co-spectrum should be much stronger than the velocity quadrature spectrum of two vertically separated probes. This is indeed the case as shown by our measurements in the turbulent wake of a cylinder in a homogeneous fluid (water), Fig. 12a. The coherency measurements, Fig. 12b, show that there were no identifiable coherent frequencies in the flow. However, in a stratified wake with internal waves (Run WSF-2), our velocity measurements show that, from two vertically separated probes, the quadrature-spectrum is no longer small compared with the co-spectrum (Fig. 13a) and the signals are coherent at distinct frequencies (Fig. 13b). Similar behaviors are shown in the co-spectra, quadrature-spectra, and coherencies of two vertically separated concentration probes (Figure 14a

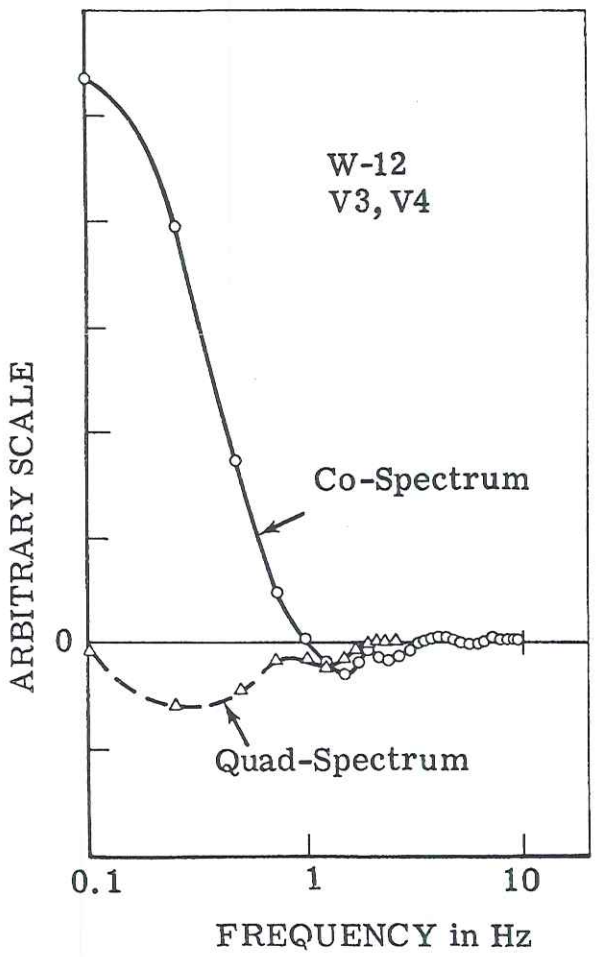

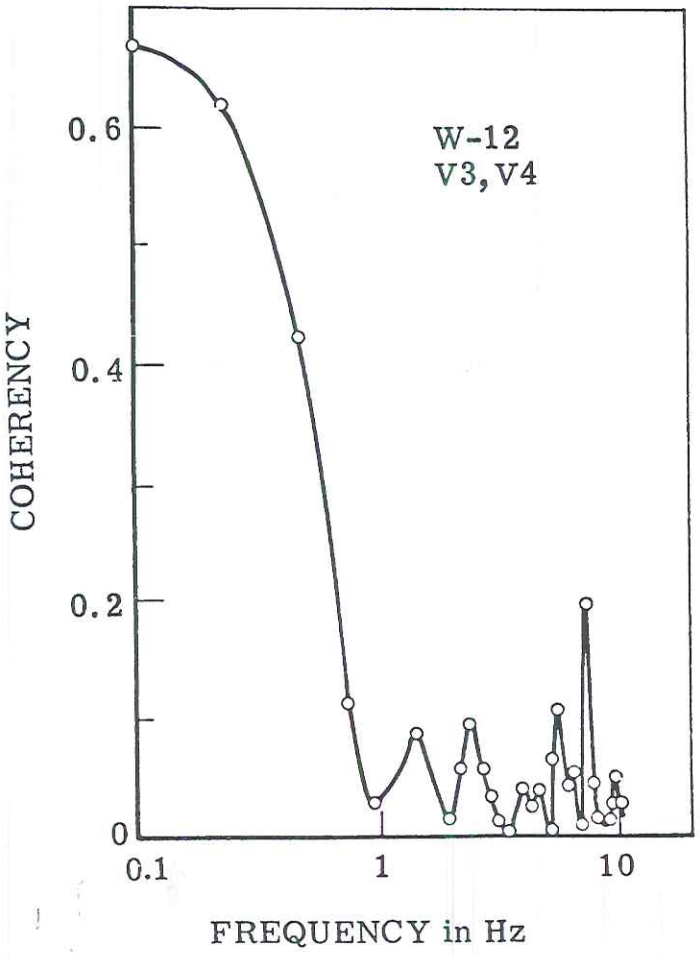

Fig. 12. Velocity cross-spectra of two vertically separated probes measured in a homogeneous wake (Run W-12). Vertical separation of the probes = 2.54 cm (z/D = 1). V3 probe is at x/D = 20, and z/D = 0. V4 probe is at x/D = 20 and z/D = 1. (See Fig. 10 for detailed description).

(a) co- and quadrature-spectra

(b) coherency

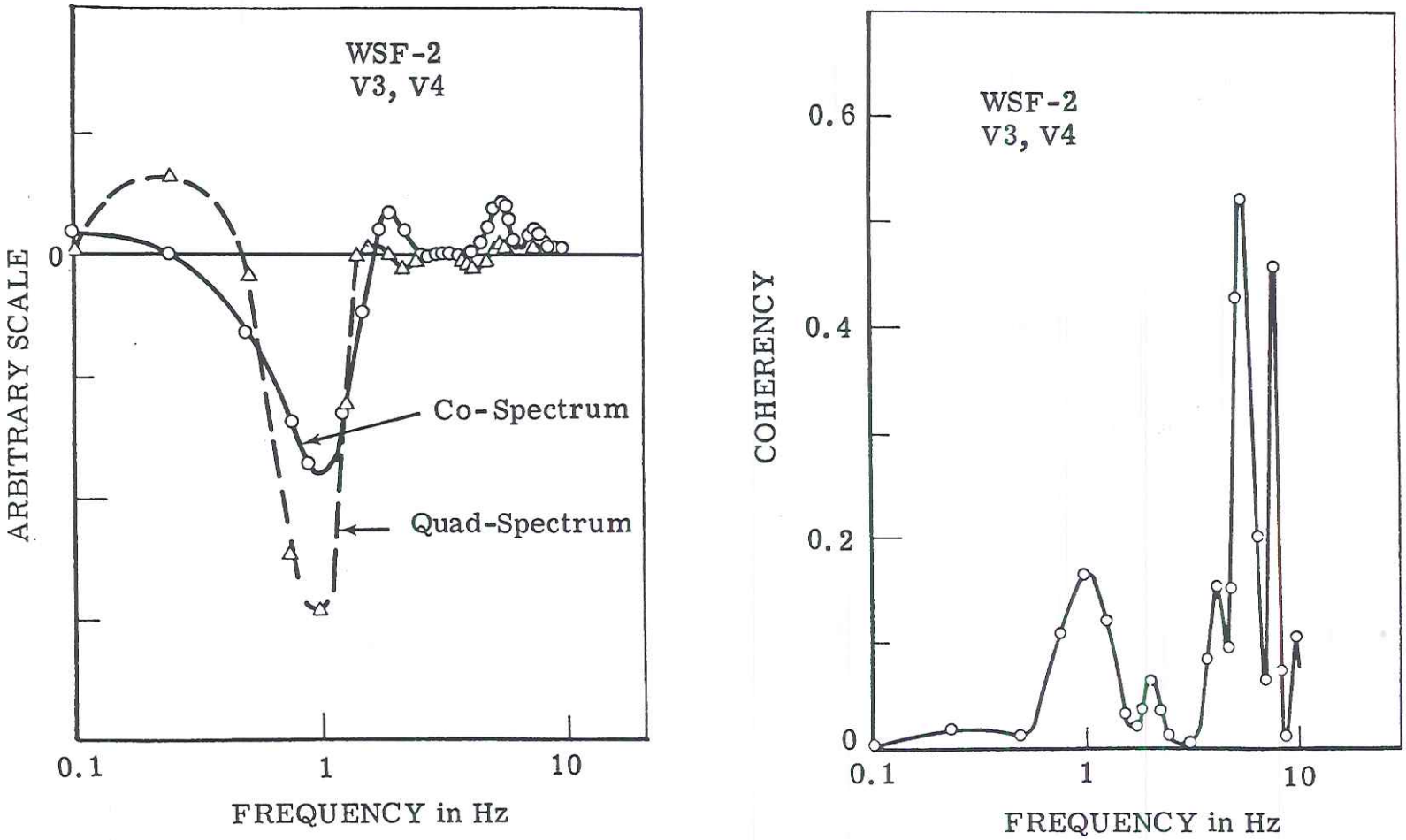

Fig. 13. The velocity cross-spectra of two vertically separated probes measured in a stratified wake (Run WSF-2). Vertical separation of the probes is 2.54 cm. V3 is at x/D = 20 and z/D = 0. V4 is at x/D = 20 and z/D = 1. (See Fig. 11 for detailed description).

(a) co- and quadrature-spectra

(b) coherency

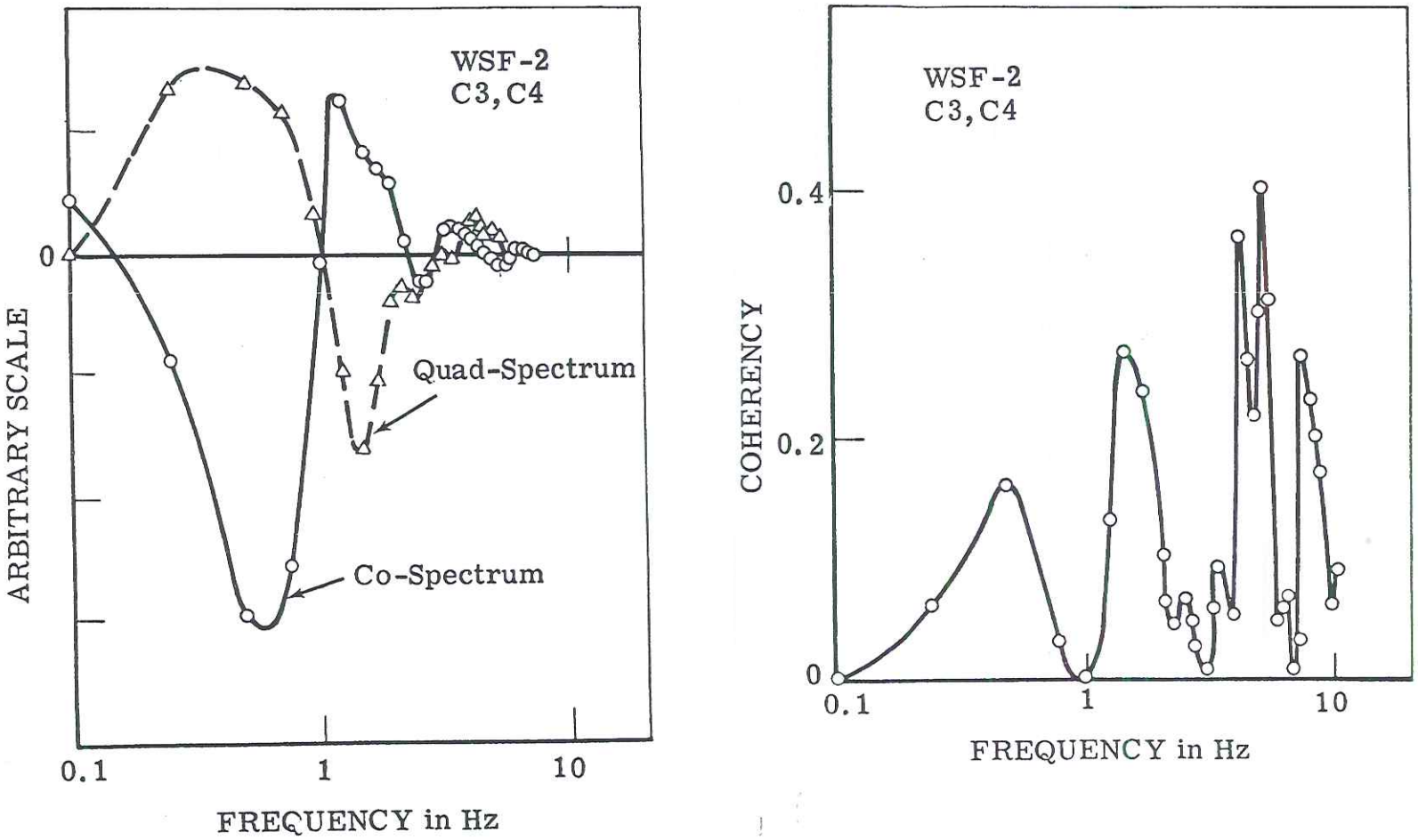

Fig. 14. The concentration cross-spectra of two vertically separated probes measured in a stratified wake (WSF-2). Vertical separation of the probes is 2.54 cm. C3 is at x/D = 20 and z/D = 0. C4 probe is at x/D = 20 and z/D = 1. (See Fig. 11 for detailed description).

(a) co- and quadrature-spectra

(b) coherency

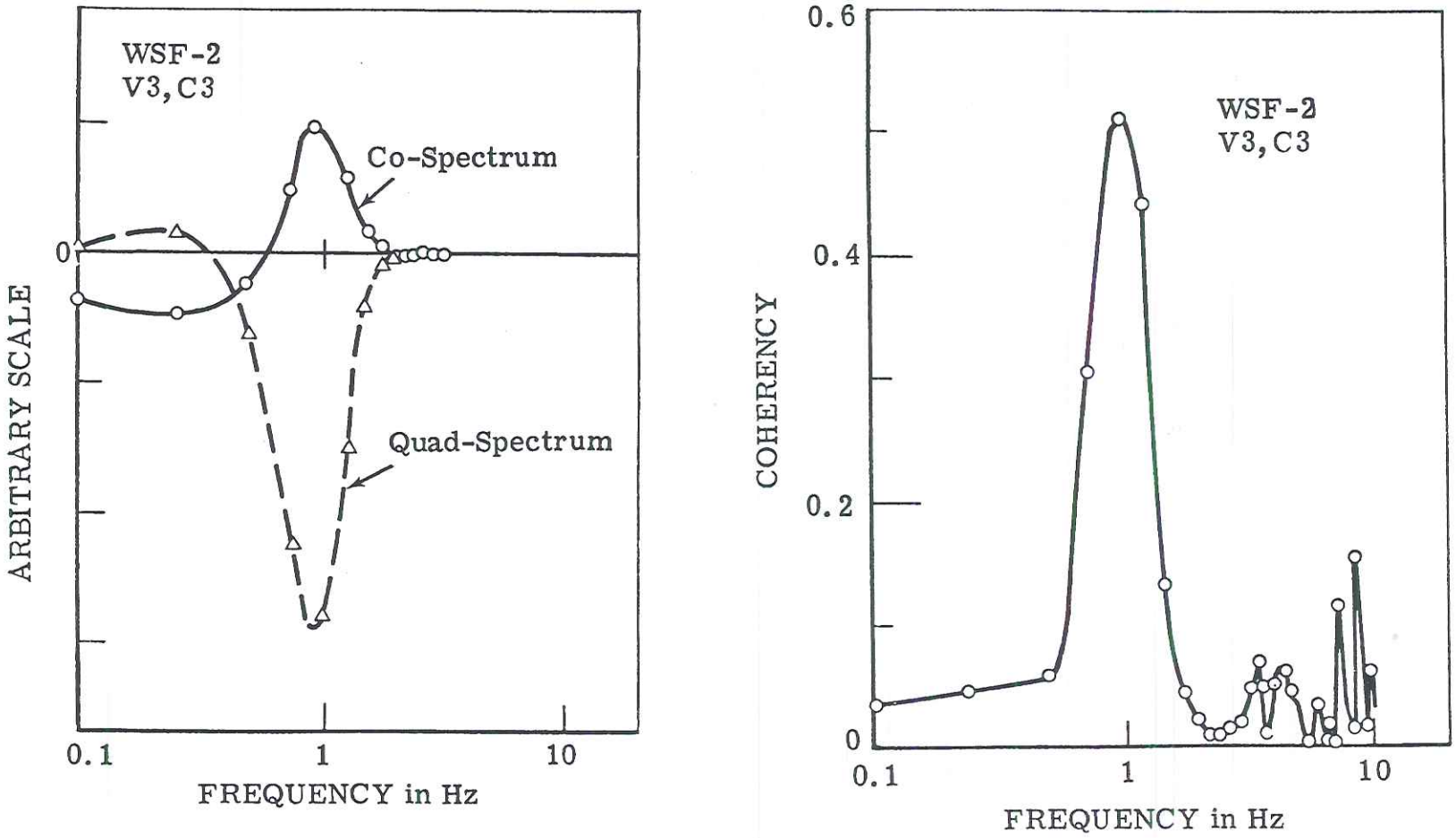

Fig. 15. The velocity and concentration cross-spectra of two horizontally separated probes in a stratified wake(Run WSF-2).
The hot-film probe V-3 and the conductivity probe C3 are at x/D=20 and z/D=0. The two probes were placed at the same height but separated horizontally at 1.7 cm (See Fig. 11 for detailed description).

(a) co- and quadrature spectra
(b) coherency

and 15b) or of a velocity probe and a concentration probe (Figure 15a and 15b). These characteristics can be used to detect whether there are internal waves present in a turbulent flow and to identify the frequency range in which internal waves dominate.

There is another way to look at the diagnostic method proposed above. A fluctuating component can be expressed in terms of amplitude and phase. We assume that strong phase relation may exist between measurements at two vertically separated probes if there are internal waves present (at least this is true from small disturbance theory), and we propose to measure the spectra that are representative of the phase relation -- the co- and the quadrature-spectra.

This diagnostic method, we believe, can be used to distinguish waves from turbulence in the atmosphere or ocean. It would be interesting to test this method in the atmosphere from a tower by measuring the co- and quadrature spectra of two vertically separated velocity and/or temperature probes under different stably and unstably stratified atmospheric conditions.

Acknowledgements

The author wishes to thank Mr. S. D. Hansen for his help in developing the digital data processing program, and Mr. R. L. Carlsen and Mr. T. E. Maupin for their help in the experimental work. He is indebted to Miss Edna R. Holmes for typing the manuscript.

Run	Speed Control Pot Setting	Actual Speed in cm/sec.
Cal. 1	3.00	13.981
Cal. 2	3.00	13.989
Cal. 3	3.00	13.981
Cal. 4	3.00	13.970
Cal. 5	3.00	13.965
Cal. 6	3.00	13.945
Cal. 7	3.00	13.974
Cal. 8	3.00	13.996
Cal. 9	3.00	13.953
Cal. 10	3.00	13.992

Table I

Speed Repeatability of the Towing System

Towing Speed in cm/sec	rms Vibration Velocity/Mean Velocity
14	3.07%
22	0.92%
25	1.34%
36	0.79%
42	0.61%

Table II

Carriage Vibration as Recorded

by a Hot-film Cone Probe

(cable tension: 85 lb/in^2; air pressure: 45 lb/in^2)

References

Bolgiano, R. (1959), Turbulent spectra in a stably stratified atmosphere, *J. Geophy. Res.*, 64 (12), 2226-2229.

Bolgiano, R. (1962), Structure of turbulence in stably stratified media, *J. Geophy. Res.*, 67 (8), 3015-3023.

Fabula, A. G. (1968), Operating characteristics of some hot-film velocity sensors in water. Advances in Hot-Wire Anemometry, Ed. by W. L. Melnik & J. R. Weske, Department of Aero. Eng., Univ. of Maryland, College Park, Md.

Gibson, C. H., & Schwarz, W. H. (1963), Detection of conductivity fluctuations in a turbulent flow field, *J. Fluid Mech.*, 16, 357-364.

Hall, J. M., & Pao, Y.-H. (1969), Spectra of internal waves and turbulence in stratified fluids, 2, Experiments on the breaking of internal waves in a two-fluid system, *Radio Sci.*, 4(12), 1321-1325.

Hardy, K. R., Glover, K. M., & Otterstem, H. (1969), Radar investigations of atmospheric structure and CAT in the 3 to 20-km region, Clear Air Turbulence and Its Detection, Ed. by Y.-H. Pao and A. Goldburg, Plenum Press, N. Y., N. Y.

Kennedy, F. J. & Froebel, R. A. (1964), Two-dimensional turbulent wakes in density-stratified liquids, ASME Publication, 64-WA/UNT-11.

Kolmogorov, A. N. (1941), The local structure of turbulence in an incompressible fluid at very large Reynolds numbers, *Proc. Acad. Sci. USSR*, 30 (4), 301-305.

Long, R. R. (1955), Some aspects of the flow of stratified fluids, III. Continuous density gradients, *Tellus*, 3, 341-357.

Long, R. R. (1954), Some aspects of the flow of stratified fluids, II. Experiments with a two-fluid system, *Tellus*, 2, 97-115.

Long, R. R. (1953), Some aspects of the flow of stratified fluids. I. Theoretical investigation, *Tellus*, 1, 42-58.

Lumley, J. L. (1964), The spectrum of nearly inertial turbulence in a stably stratified fluid, *J. Atmos. Sci.*, 21 (1), 99-102.

Pao, Yih-Ho (1965), Structure of turbulent velocity and scalar fields at large wavenumbers, *Phys. Fluids*, 8 (6), 1063-1075.

Pao, Yih-Ho,(1967), Turbulence in stratified fluids (abstract), Proc. IUGG/IUTAM Int. Symp. on Boundary Layers and Turbulence including Geophysical Applications, September 19-24, 1966, Kyoto, Japan, *Phys. Fluids*, 10 (9), part 2, S311.

Pao, Yih-Ho (1968a), Turbulent velocity and scalar spectra in stably stratified fluids (summary), *Informal Report on the Symposium on Theoretical Problems in Turbulence Research*, September 9-13, 1968, University Park, Pa., Ed. by H. Tennekes. Also Boeing Docu. D1-82-0680, Seattle, Washington.

Pao, Yih-Ho (1969a), Origin and structure of turbulence in stably stratified media, in Clear Air Turbulence and Its Detection, Ed. by Yih-Ho Pao and Arnold Goldburg, pp. 73-99, Plenum Press, New York.

Pao, Yih-Ho (1969b), Spectra of internal waves and turbulence in stratified fluids, 1, General discussion and indications from measurements in stably stratified atmosphere and ocean, *Radio Sci.*, 4, 1315-1320.

Pao, Yih-Ho, Hansen, S. D., MacGregor, G. R. (1969), On-Line computer analysis of turbulence data with the fast Fourier transform method, Boeing Docu. D1-82-0863, Seattle, Washington.

Schooley, A. H. & Stewart, R. W. (1963), Experiments with a self-propelled body in a fluid with a vertical density gradient, *J. Fluid Mech.*, 9 (1).

Stockhausen, P. J., Clark, C. B., Kennedy, J. F. (1966), Three-dimensional momentumless wakes in density stratified liquids. Hydrodynamics Laboratory Rept. No. 93, Dept. of Civil Engineering, Mass. Inst. of Tech., Cambridge, Mass.

U.S. DEPARTMENT OF COMMERCE
Technology Administration
National Technical Information Service
Springfield, VA 22161 (703) 605-6000